

Transition metal doped TiO₂ thin films epitaxially grown by reactive sputter deposition

B.-S. Jeong¹, Y.W. Heo¹, J. D. Budai², Y. D. Park³, and D. P. Norton¹

¹University of Florida, Dept. of Materials Science and Engineering, 100 Rhines Hall, P.O.

Box 116400, Gainesville, FL 32611, U.S.A.

²Oak Ridge National Laboratory, Solid State Division, Oak Ridge, TN 37831, U.S.A.

³Seoul National University, School of Physics, Seoul 151-747, Korea

Abstract

In recent years, ferromagnetic semiconductors have been extensively explored as potential candidates for spin injection in spin electronic devices operating at room temperature. In this report, transition metal(TM) doped TiO₂ thin films were epitaxially grown by reactive magnetron sputtering. X-ray diffraction pattern indicates that these TM doped thin films are single crystal-like anatase films. Field emission SEM shows that surface segregation of Co was observed in the film for the 7 at% Co-doped TiO₂ anatase films. The resistivity and carrier concentration for Co_{0.07}Ti_{0.93}O₂ was 7.18Ω-cm and 8.09×10^{17} . This semiconductor material was N-type. The hysteresis of this material shows the strong ferromagnetic behavior at room temperature.

INTRODUCTION

There is considerable interest in realizing spin-based semiconductor electronic devices involving the exploitation of spin-polarized electron distributions in dilute magnetic semiconductor (DMS) materials. In most semiconductors doped with transition metals, the magnetic behavior, if any, is observed at temperatures well below room temperature [1-5]. For (Ga, Mn)As, a Curie temperature (T_c) as high as 110K has been reported [6-7]. However, the recent report that cobalt-doped semiconducting anatase (TiO_2) is ferromagnetic at room temperature opens the possibility of developing non-cryogenic spin-based DMS electronics [8]. Ferromagnetic thin films of $\text{Co}_x\text{Ti}_{1-x}\text{O}_2$, epitaxially stabilized in the anatase structure, is possible on $\text{SrTiO}_3(001)$ and $\text{LaAlO}_3(001)$ [9]. Spectroscopic studies on these samples grown by oxygen plasma assisted molecular-beam epitaxy (OPA-MBE) suggests that the cobalt exists in the Co^{2+} oxidation state in the MBE-grown TiO_2 thin films, consistent with ferromagnetism originating from Co substitution on the Ti site. However, other studies of Co-doped TiO_2 films deposited by pulsed laser deposition (PLD) suggest that the formation of Co nanoclusters may be responsible for the ferromagnetic properties [10]. Thus, it remains an open question as to the origin of ferromagnetism in these materials, as well as the probable role that the specific processing technique plays in yielding these results.

In this talk, we discuss the growth and properties of Co-doped $\text{TiO}_2(\text{Co}_x\text{Ti}_{1-x}\text{O}_2)$ epitaxial thin films realized by reactive co-sputter deposition. The use of a water vapor (H_2O) as the oxidant facilitates the formation of carriers via the creation of oxygen vacancies. The growth and properties of undoped semiconducting in transparent anatase

TiO₂ thin films epitaxially grown by reactive sputtering deposition employing water vapor have been reported elsewhere[11].

EXPERIMENTAL DETAILS

$\text{Co}_x\text{Ti}_{1-x}\text{O}_2$ anatase films were epitaxially grown by a reactive RF magnetron co-sputter deposition with cation sputtering targets of Ti (99.995%) and Co(99.95%). The film-growth system was equipped with multiple 2" sputtering sources and a load-lock for substrate exchange. The base pressure of the deposition system was on the order of 5×10^{-8} Torr. For epitaxially stabilized anatase TiO_2 film growth, (001) LaAlO_3 was chosen as the substrate as it provides a lattice mismatch on the order of 2 at%. The substrates were cleaned with solvents prior to loading on the sample holder. Argon was provided as the sputter gas. A water source was created by freezing and evacuating a water-filled stainless cylinder that was attached to the deposition chamber via a leak valve. The total pressure during growth was fixed at 15mTorr, whereas the water vapor pressure was varied from 10^{-4} and 10^{-2} Torr. A water vapor pressure of $P(\text{H}_2\text{O})=10^{-3}$ Torr was found to be optimal in realizing oxygen deficiency and semiconductor transport behavior. A substrate temperature during the deposition of 650°C resulted in the growth of highly crystalline epitaxial Co-doped TiO_2 thin film in the anatase phase. The growth rate was 1.9nm/min.

The crystalline structure of Co-doped TiO_2 films was characterized by X-ray diffraction (XRD) with a Cu K α radiation source. Quantitative analysis of chemical composition was performed by electron probe microanalysis (EPMA). In order to extract information regarding chemical states of the element, X-ray photoelectron spectroscopy (XPS) was used with Al-K α radiation ($h\nu=1486.6\text{eV}$). The surface morphology, back-scattered images and chemical mapping, were performed by field emission scanning electron microscopy (FESEM). Hall effect measurements were performed to measure

transport properties of oxygen-deficient Co-doped TiO₂ anatase films. Room temperature M-H loops were measured by a Quantum Design superconducting quantum interference device (SQUID) magnetometer for films with different Co content ($x=0.07, 0.02$).

RESULTS AND DISCUSSION

The Co-doped epitaxial anatase films realized for a growth temperature of 650°C and water vapor pressure at 10⁻³Torr exhibited crystalline quality similar to that seen in previous work on undoped films [12]. Fig.1. shows the θ -2 θ X-ray diffraction data taken along the surface normal for films deposited under these conditions with 7 at% and 44 at% Co doping levels. For the 7 at% Co-doped TiO₂, the films are near single phase epitaxial anatase with a small amount of secondary rutile phase seen in the data. However, 44 at% Co-doped TiO₂ films show epitaxially stabilized anatase TiO₂ without rutile phase. For both 7 at% and 44 at% Co-doped TiO₂ films, as shown in Fig. 1, there was no evidence for metallic Co or cobalt oxides phases seen in the diffraction data. There is little difference observed for the X-ray diffraction patterns from the two films.

In order to investigate transport properties of the Co-doped anatase films, Hall effect measurement at room temperature was performed. The current used for the measurement was 100 μ A. The 7 at% Co-doped TiO₂ thin films shows n-type semiconductor behavior. The carrier concentration was typically in the range of 10¹⁷-10¹⁸cm⁻³, which is lower than that shown for MBE-grown films [13]. The resistivity of the 7 at% Co-doped thin film is slightly higher than undoped anatase films. However, the 44 at% Co-doped anatase films show insulator behavior. This is consistent with a previous paper reporting the relationship between carrier mobility and concentration of

dopants [14]. B. -S. Jeong *et al.* showed that the carrier mobility decreases as the cobalt concentration increased. According to these results, the carrier mobility of the 7 at% Co-doped TiO₂ was 1cm²/Vs, indicating that over the 7 at% of Co content, the carrier mobility may be less than 1cm²/Vs, showing insulating behavior which has very low carrier mobility.

Fig. 2 shows the magnetization properties of the Co-doped thin film plotted as a magnetization(M)-Applied field(H). Each sample has the same size as 5mm×5mm×1mm. The sample thickness for both Co-doped anatase films is 300nm for 2hrs sputter deposition time. For both the 7 at% and 44 at% Co-doped TiO₂ sample, hysteresis loops are observed at room temperature for film grown at 650°C with water vapor as a oxidant. The magnetic saturation (Ms) for the 7 at% and 44 at% Co-doped thin films is 11.30 (emu/cm³) and 2.6(emu/cm³), respectively. Although the 44 at% Co-doped anatase has much more Co to potentially contribute to the ferromagnetic moment, the 7 at% Co-doped TiO₂ film clearly exhibits stronger ferromagnetic behavior relative to the 44 at% doped thin films.

The elemental composition for the 7 at% Co-doped TiO₂ thin films was determined by XPS. The satellite peak structure that is observed on the high binding energy side of the principal 2p_{1/2} and 2p_{3/2} lines is indicative of high spin Co 2+ [15]. The shake-up peak is an easily identified characteristic of the chemical state of the Co [16]. The results from the XPS analysis taken from the as-grown surface is consistent with the Co existing in the +2 formal oxidation state in these sputter-deposited Co_xTi_{1-x}O₂ anatase thin films.

In order to further investigate the properties of these materials, the surface topography was determined using field-emission SEM. Fig. 3 shows the backscattered electron image obtained by the FESEM for the 7 at% and 44 at% Co-doped TiO₂ anatase thin films grown on (001) LaAlO₃. In case of the 7 at% Co-doped TiO₂, the sample surface is decorated with secondary phase precipitates. As reported elsewhere, the material of surface segregation shown in Fig. 3(a) for the Co-doped thin films is Ti-Co-O particles [14]. As shown in Fig. 3(b), however, sputter deposited Co_{0.44}Ti_{0.56}O₂ film does not show these secondary phase precipitates. Note that the 7 at% Co-doped TiO₂ films show stronger ferromagnetic behavior than the 44 at% doped anatase.

In order to further investigate the concentration of Co in TiO₂ thin films, Auger electron spectroscopy (AES) was also performed. Results from the AES, also given in Fig. 4, indicate that the 44 at% Co-doped TiO₂ thin films clearly show higher Co contents than the 7 at% Co-doped anatase films.

Fig. 5(a) and 5(b) show room-temperature atomic force microscopy (AFM) and magnetic force microscopy (MFM) images taken along the surface of the 7 at% Co-doped TiO₂ thin films, respectively. Since MFM measures the magnetic force gradient, which is proportional to the amount and strength of magnetic charges, the contrast information of the microscopic images has the same trend as the macroscopic magnetization measurement [17].

As shown in Fig. 5(a), the sample surface is covered with segregated particle, Ti-Co-O phase, consistent with FESEM data shown in Fig. 3(a). Fig. 5(b) shows the magnetic structures as bright and dark contrasts at room temperature. Note that the brighter contrast is shown on the secondary phase precipitates, indicating that these

secondary phase precipitates show stronger magnetic force than the other areas of the film. This is consistent with the Ti-Co-O phases containing more cobalt relative to other areas. This picture corresponds well to the survey of AES and EDS mapping taken by FESEM. From the surface structure and the results of magnetic measurement, we conclude that the surface segregation of Ti-Co-O phases in Co-doped TiO₂ thin films affects the ferromagnetic properties of the Co-doped anatase films.

In conclusion, we have investigated ferromagnetism in semiconducting anatase Co-doped TiO₂ thin films grown by the reactive sputter deposition technique. Surface segregation from Co oxide particles was observed in 7 at% Co-doped films. Both pure and 7 at% Co-doped films grown using water vapor source showed n-type semiconductor properties. Our results from XPS clearly show that Co is primarily in the +2 formal oxidation state in this doped thin films. From the results of surface structure and magnetic measurement, we conclude that the surface segregation existing as a Ti-Co-O phases in Co-doped TiO₂ thin films affects the ferromagnetic properties of the Co-doped anatase films. Further activities will focus on the origin of the ferromagnetism.

ACKNOWLEDGEMENT

This work was partially supported by the Army Research Office through research grant DAAD 19-01-1-1508 grant. The authors would also like to acknowledge the staff of the Major Analytical Instrumentation Center, Department of Materials Science and Engineering, University of Florida, for their assistance with this work.

REFERENCE

1. S. Datta, B. Das, *Appl. Phys. Lett.* 56, 665 (1990)
2. S. A. Wolf, D.D. Awschalom, R. A. Buhrman, J. M. Daughton, S. Von Molnar, M. L. Roukes, A. Y. Chtchelkanova, D. M. Treger, *Science* 294, 1488 (2001)
3. D. D. Awschalom, M. E. Flatté and N. Samarth, *Scientific American*, June (2002)
4. S. A. Wolf, D. D. Awschalom, R. A. Buhrman, J. M. Daughton, S. von Molnar, M. L. Roukes, A.Y. Chtchelkanova, D.M.Treger, *Science* 294, 1488(2001)
5. Y. D. Park, A. T. Hanbicki, S. C. Erwin, C. S. Hellberg, J. M. Sullivan, J. E. Matson, T. f. Ambrose, A. Wilson, G. Spanos, B. T. Jonker, *Science* 295, 651 (2002)
6. H. Ohno, F. Matskura, T. Omiya, and N. Akiba, *J. Appl. Phys.* 85, 4277(1999)
7. H. Ohno, A. Shen, F. Matsukura, A. Oiwa, A. Endo, S. Katsumoto, Y. Iye, *Appl. Phys. Lett.* 69(3), 363(1996)
8. Y. Matsumoto, M. Murakami, T. Shono, T. Hasegawa, T. Fukumura, M. Kawasaki, P. Ahmet, T. Chikyow, S.-Y. Koshihara, H. Koinuma, , *Science* 291, 854(2001)
9. S. A. Chambers, C. M. Wang, S. Thevuthasan, T. Droubay, D. E. McCready, A. S. Lea, V. Shutthanandan and C. F. Windisch Jr ,*Thin Solid Films* 418, 2, 197(2002)
10. D. H. Kim, J. S. Yang, K.W. Lee, S. D. Bu, T.W. Noh, S.-J. Oh, Y.-W. Kim, J.-S. Chung, H. Tanaka, H. Y. Lee, and T. Kawai, *Appl. Phys. Lett* 81, 2421(2002)
11. B.-S. Jeong, D. P. Norton, J. D. Budai, *Solid-State Electronics*, (2003)(In press)
12. B.-S. Jeong, J.D. Budai, D.P. Norton, *Thin Solid Films* 422, 166 (2002)
13. S.A.Chambers, S. Thevuthasan, R.F.C. Farrow, R.F.Marks, J. U. Thiele, L. Folks, M.G. Samant, A. J. Kellock, N. Ruzycski, D. L. Ederer, and U. Diebold, *Appl. Phys. Lett.* 79, 3457(2001)
14. B.-S. Jeong, Y. W. Heo, J. D. Budai, Y. D. Park, and D. P. Norton, (unpublished)
15. *Handbook of X-ray photoelectron spectroscopy*, physical electronics, (1995).
16. S. N. Towle, J. R. Bargar, G. E. Brown, Jr., and G. A. Parks, *J. Colloid. Interface*
17. S. H. Chung, S. R. Shinde, S. B. Ogale, A. Biswas, T. Venkatesan, R. L. Greene, M. Dreyer, J. B. Drottellis, A. Millis, and R. D. Gomez, *IEEE Trans. on magnetics*, 38(5), 2886(2002)

Figure Captions:

Fig. 1 The X-ray diffraction pattern for $\text{Co}_x\text{Ti}_{1-x}\text{O}_2$ on $\text{LaAlO}_3(001)$ ($x=0.07, 0.44$)

Fig. 2 An M-H curve for $\text{Co}_x\text{Ti}_{1-x}\text{O}_2$ ($x=0.07, 0.44$) thin films on $\text{LaAlO}_3(001)$ taken at room temperature. Magnetic field was applied parallel to the film surface.

Fig. 3 Backscattered(BS) image for the $\text{Co}_x\text{Ti}_{1-x}\text{O}_2$ ($x=0.07, 0.44$) thin films on $\text{LaAlO}_3(001)$: (a) BS image of $\text{Co}_{0.07}\text{Ti}_{0.93}\text{O}_2$, (b) BS image of $\text{Co}_{0.44}\text{Ti}_{0.56}\text{O}_2$

Fig. 4 AES survey for the surface of $\text{Co}_x\text{Ti}_{1-x}\text{O}_2$ ($x=0.07, 0.44$) on $\text{LaAlO}_3(001)$: (a) AES survey of $\text{Co}_{0.07}\text{Ti}_{0.93}\text{O}_2$, (b) AES survey of $\text{Co}_{0.44}\text{Ti}_{0.56}\text{O}_2$

Fig. 5 Atomic force microscopy (AFM) and Magnetic force microscopy (MFM) images for the $\text{Co}_{0.07}\text{Ti}_{0.93}\text{O}_2$: (a) AFM image, (b) MFM image

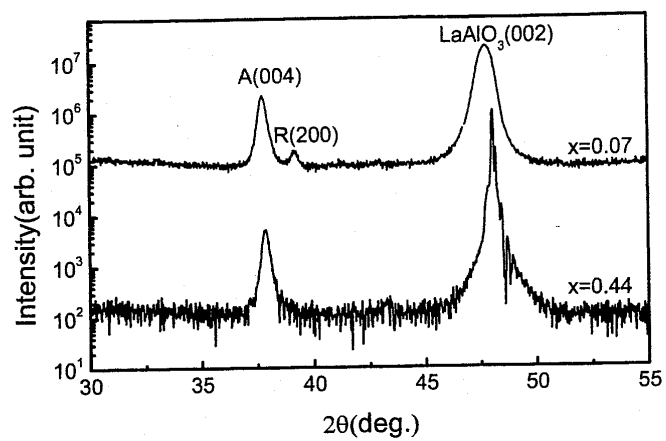


Fig. 1

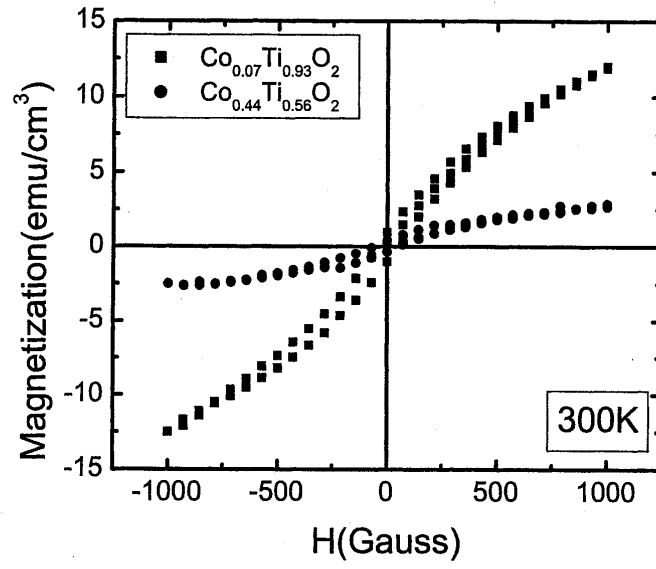


Fig. 2

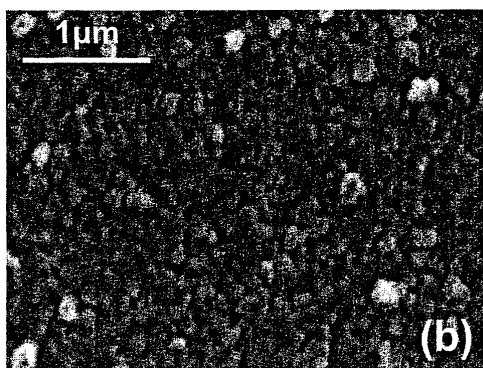
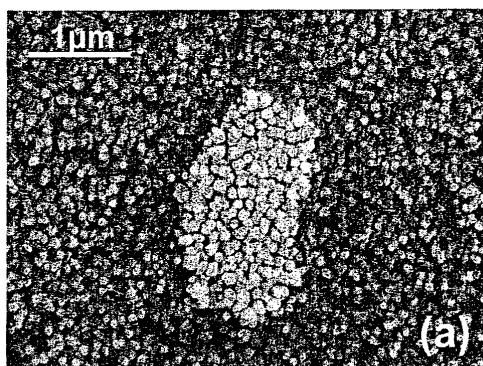


Fig. 3.

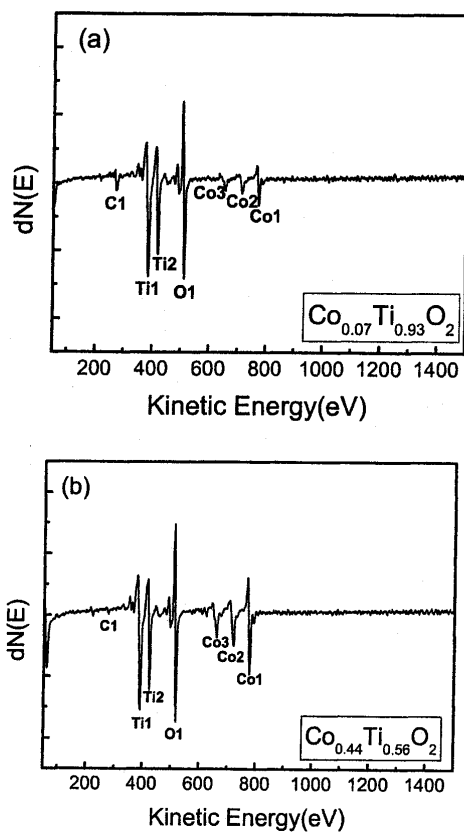


Fig. 4

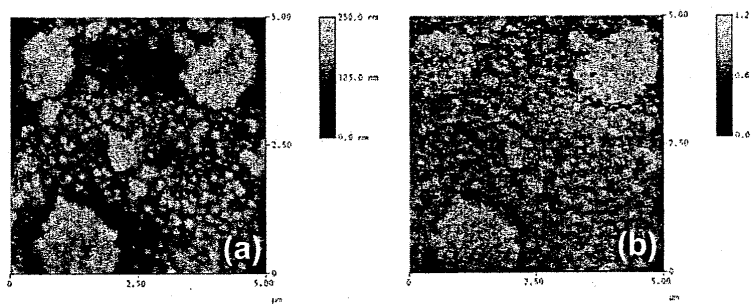


Fig. 5.